Effects of Mutations on the Partitioning of DNA Substrates between the Polymerase and 3′−5′ Exonuclease Sites of DNA Polymerase I (Klenow Fragment)†

Wai-Chung Lam,‡ Edwin J. C. Van der Schans,‡ Catherine M. Joyce,§ and David P. Millar*,‡

Department of Molecular Biology, MB-19, The Scripps Research Institute, 10550 North Torrey Pines Road, La Jolla, California 92037, and Department of Molecular Biophysics and Biochemistry, Yale University, New Haven, Connecticut 06520

Received August 13, 1997; Revised Manuscript Received November 17, 1997

ABSTRACT: Site-directed mutagenesis and time-resolved fluorescence spectroscopy were used to evaluate the contributions of individual amino acid side chains to the binding of DNA primer−templates to the 3′−5′ exonuclease site of the large proteolytic fragment (Klenow fragment) of DNA polymerase I. Mutations were introduced into side chains that have been shown crystallographically to be in close proximity to a DNA 3′ terminus bound at the 3′−5′ exonuclease site. The wild-type residues were replaced by alanine in each case. To assess the effects of the mutations on DNA binding, time-resolved fluorescence anisotropy measurements were performed on dansyl-labeled primer−templates bound to the mutant enzymes. In contrast to techniques that simply monitor the overall binding of proteins to DNA, the time-resolved fluorescence anisotropy technique was used to determine the fractional occupancies of the polymerase and 3′−5′ exonuclease active sites of Klenow fragment. Equilibrium constants describing the partitioning of DNA between the two active sites were obtained for nine different mutant enzymes bound to both matched and mismatched DNA sequences. Mutations of Leu361 and Phe473 caused the largest effects, significantly destabilizing the binding of mismatched DNA substrates to the 3′−5′ exonuclease site relative to DNA bound at the polymerase site, consistent with structural data showing that the side chains of these residues are involved in intimate hydrophobic interactions with the 3′ terminal and penultimate bases of the primer strand [Beese, L., and Steitz, T. A. (1991) *EMBO J. 10*, 25−33]. Mutations of the His660 and Glu357 side chains also resulted in significant effects on the binding of mismatched DNA to the 3′−5′ exonuclease site. Surprisingly, mutation of Tyr497 increased the partitioning of mismatched DNA into the 3′−5′ exonuclease site, suggesting that the tyrosine side chain in the wild-type enzyme destabilizes substrate binding, despite crystallographic data showing that Tyr497 is H-bonded to the DNA substrate. The effects of mutating the amino acid side chains that serve as ligands to two divalent metal ions bound at the 3′−5′ exonuclease site, designated A and B, indicated that metal A also helps to bind DNA to the 3′−5′ exonuclease site. These results demonstrate that the time-resolved fluorescence anisotropy technique can be used to quantify the energetic contributions associated with each of the crystallographically defined DNA−protein contacts at the 3′−5′ exonuclease site.

The Klenow fragment of DNA polymerase I has two separate enzymatic activities, a 5′−3′ polymerase activity that is used to extend a nascent DNA strand during DNA replication and a 3′−5′ exonuclease activity that acts in opposition to the polymerase activity and is used to edit misincorporated nucleotides. Klenow fragment is an attractive model system for structure−function studies of a DNA replication enzyme, owing to the availability of high-resolution crystal structures of the enzyme and its complexes with DNA substrates (reviewed in ref *1*). The active sites for the polymerase and 3′−5′ exonuclease reactions are located in separate structural domains of the protein and are separated by about 35 Å (*2*−*4*), indicating that there must be two different binding modes for a DNA primer−template depending on whether the enzyme is carrying out DNA polymerization or an editing reaction. The mechanisms that determine whether a DNA substrate will occupy one or the other of the two active sites are not well understood. In this paper, we present a detailed study of the amino acid side chains that are involved in the binding of DNA to the 3′−5′ exonuclease site of Klenow fragment.

Early biochemical studies of Klenow fragment indicated that the preferred substrate for the 3′−5′ exonuclease activity was single-stranded DNA (*5*), implying that the enzyme was capable of melting the primer terminus while carrying out an editing reaction on a double-stranded DNA substrate. This proposal subsequently was confirmed by structural studies of crystalline complexes of Klenow fragment with single-stranded and duplex DNA substrates (*3*, *6*) and by solution studies employing chemically cross-linked duplex DNA substrates (*7*). These studies indicated that the exonuclease site melts out the last four base pairs at the primer 3′ terminus of a duplex DNA substrate. Time-resolved fluorescence spectroscopic studies of oligonucleotide duplexes containing the fluorescent nucleotide analogue 2-aminopurine also have been used to monitor the melting of a DNA duplex terminus

† Supported by the National Institutes of Health (Grants GM44060 to D.P.M. and GM28550 to C.M.J.).

* Corresponding author.
‡ The Scripps Research Institute.
§ Yale University.

S0006-2960(97)02018-7 CCC: $15.00
Published on Web 01/22/1998

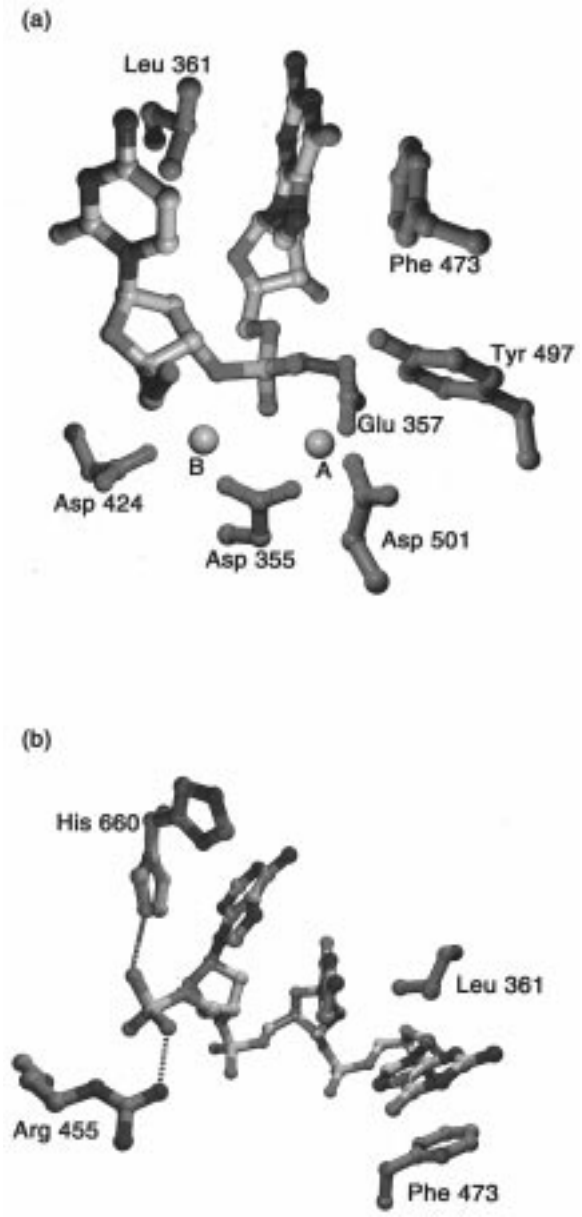

FIGURE 1: Important side chains at the 3′−5′ exonuclease active site of Klenow fragment (*9*). (a) A bound dinucleotide at the 3′−5′ exonuclease active site. The dinucleotide is shown in gray, with the phosphorus at the scissile phosphodiester in pink. The protein side chains illustrated are those that interact with the substrate or that serve as metal ligands. The two divalent metal ions at the active site are represented by the spheres marked A and B. (b) A more distant view of three residues of single-stranded DNA bound to the exonuclease region. The view is rotated relative to that of panel a, as can be seen from the positions of the Leu361 and Phe473 side chains. The His660 side chain has two conformations in the presence of bound DNA: The major conformation (green) interacts with the third base from the 3′ end, and the minor conformation (cyan) forms a hydrogen bond to the third phosphate (also illustrated is Arg455, which interacts with the third phosphate; this residue was not part of this study). Other side chains interacting with the phosphodiester backbone have been omitted for clarity. This illustration was created by Chad Brautigam using the program VMD (*27*) and was rendered using POV-Ray.

induced by Klenow fragment (*8*). The ability of the exonuclease site to melt an extended region of duplex DNA at its 3′ terminus raises interesting questions about the interactions that are involved in binding the resulting single-stranded bases to the exonuclease site, because these interactions necessarily must be more favorable in stabilizing the single-stranded region of DNA than the base−base interactions that stabilize the duplex.

Crystallographic studies of Klenow fragment−DNA complexes have provided considerable information on the DNA−protein interactions at the 3′−5′ exonuclease site. A crystal structure of Klenow fragment complexed with a tetranucleotide identified the amino acid side chains that form the 3′−5′ exonuclease active site and revealed many of the interactions between the protein and the DNA substrate (*3*, *9*) (Figure 1). The structural data define an extended single-stranded DNA binding pocket, formed by a group of side chains that make hydrophobic contacts with the unstacked nucleotide bases or are hydrogen-bonded to the sugar−phosphate backbone. A structure of an editing complex of Klenow fragment with an 11-base pair duplex DNA substrate containing a 3′ overhanging single strand showed that the 3′ terminus was bound to the 3′−5′ exonuclease site in a fashion identical to that seen in the tetranucleotide complex, with the duplex portion of the substrate occupying a cleft between the polymerase and exonuclease domains (*6*). This cleft also appears to be used in the polymerase mode of binding (*10*). In addition to the side chains involved in DNA−protein contacts, the crystallographic studies of Klenow fragment also have identified two binding sites for divalent metal ions within the 3′−5′ exonuclease site, designated A and B (*4*, *9*). Experiments in which the amino acid side chains that serve as the metal ligands were removed from the active site by site-directed mutagenesis have established the importance of both metals in the 3′−5′ exonuclease reaction (*4*, *11*).

While the crystallographic studies have identified many of the DNA−protein contacts at the 3′−5′ exonuclease site, they do not provide any information on the energetics of these interactions or indicate which side chains are the most important for binding the DNA substrate. To evaluate the energetic contributions of the crystallographically defined DNA−protein contacts, we have used a series of mutant derivatives of Klenow fragment in which individual amino acid residues at the 3′−5′ exonuclease site were replaced by alanine. The resulting mutant proteins were characterized by means of time-resolved fluorescence anisotropy measurements employing dansyl-labeled primer−template oligonucleotides as substrates for the enzyme. In a previous study, we demonstrated that the fluorescence anisotropy decay of a dansyl probe site-specifically attached to DNA can be uniquely analyzed in terms of two environments for the dansyl probe, corresponding to the polymerase and exonuclease modes of binding (*12*). The nature of the two fluorescent species was confirmed by experiments with mismatched DNA substrates (*12*) and by earlier studies employing epoxy-modified substrates that bound tightly to the polymerase site (*13*). Here we have used this technique to quantify the effect of mutations on the partitioning of DNA substrates between the polymerase and 3′−5′ exonuclease sites. The resulting data are used to evaluate the energetic contributions of individual amino acid side chains to the binding of DNA at the 3′−5′ exonuclease site.

MATERIALS AND METHODS

Construction and Purification of Mutant Derivatives of Klenow Fragment. Plasmids for overproduction of Klenow

fragment derivatives having mutations in the 3′−5′ exonuclease center have been described previously (*11*, *14*). The H660A mutation, which affects a side chain from the polymerase domain, was constructed and subcloned into an overproducer plasmid following previously published procedures (*15*). Where necessary (see the text), single mutations were combined with the D424A mutation, which essentially abolishes the exonuclease activity (*4*), using standard procedures (*16*). The mutant proteins were obtained by heat induction in the host strain CJ376 (*17*) and were purified by a four-stage fractionation procedure using FPLC (Pharmacia-LKB) (*17*).

Oligonucleotide Synthesis and Labeling. Oligonucleotides were synthesized on an automated DNA synthesizer (Pharmacia Gene Assembler Plus) using standard β-cyanoethyl phosphoramidite chemistry, and purified by reverse phase HPLC using an acetonitrile/triethylammonium acetate eluant system. To prepare dansyl-labeled oligonucleotides, a protected 5-(propylamino)deoxyuridine residue was introduced during automated synthesis and subsequently was deprotected and labeled with dansyl chloride, as described previously (*18*).

Sample Preparation. Before each measurement, 4 μM dansyl-labeled 17-mer and 4.5 μM 27-mer oligonucleotides were mixed in a buffer of 50 mM Tris (pH 7.5) and 3 mM $MgCl_2$, heated at 80 °C for 10 min, and then allowed to cool slowly to room temperature. Klenow fragment was then added to a final concentration in the range of 5−12 μM. For each DNA−protein complex, sufficient Klenow fragment was added to ensure that the DNA was fully bound, as determined by measurements of the fluorescence anisotropy decay as a function of added protein. The higher protein concentrations (>5 μM) were needed to ensure complete binding of DNA substrates containing two or three consecutive mismatched base pairs.

Time-Resolved Fluorescence Spectroscopy. Fluorescence decay measurements were performed using the time-correlated single photon counting setup described in detail elsewhere (*13*). Samples were measured in quartz cuvettes and excited at 318 nm using the frequency-doubled output from a synchronously mode-locked and cavity-dumped DCM dye laser (Coherent 702). Sample emission was collected at right angles to the excitation beam, passed through a motor-controlled polarizer, and focused on the entrance slit of a monochromator (JY H-10). The dansyl emission was monitored at 535 nm. The output from the monochromator was detected by a microchannel plate photomultiplier (Hamamatsu R2809U-01) and processed using standard time-correlated single photon counting electronics (Ortec and Tennelec). Decays were recorded in 512 channels of a multichannel analyzer (Ortec Norland 5510) using a sampling time of 88 ps per channel. For measurement of fluorescence anisotropy decay, the emission polarizer was alternated between vertical and horizontal directions every 30 s, and the decays collected with each polarizer setting were accumulated in separate memory segments of the multichannel analyzer. Movement of the polarizer and data accumulation in the multichannel analyzer were under computer control. All measurements were performed at 20 °C. Time-resolved emission data were transferred to a Sparc LX workstation for analysis.

Data Analysis. The time-dependent fluorescence anisotropy, $r(t)$, was computed from polarized components of the time-resolved fluorescence according to eq 1:

$$r(t) = \frac{I_{||}(t) - I_{\perp}(t)}{I_{||}(t) + 2I_{\perp}(t)} \tag{1}$$

where $I_{||}(t)$ and $I_{\perp}(t)$ are the intensity decays measured with the emission polarizer oriented parallel or perpendicular to the excitation polarization, respectively. Previous time-resolved fluorescence studies have shown that the dansyl probe is partitioned between two distinct local environments, an aqueous environment permitting extensive local rotation and a hydrophobic environment in which rotation of the probe is markedly restricted (*12*). These environments are associated with different binding modes of the polymerase−DNA complex. Specifically, the exposed probes correspond to DNA primer−templates bound to Klenow fragment with the primer 3′ terminus in the polymerase active site, while the buried probes correspond to bound primer−templates with the 3′ terminus at the 3′−5′ exonuclease site. Therefore, the observed time-dependent anisotropy was represented by a weighted sum of contributions from the exposed dansyl probes, $r_e(t)$, and the buried probes, $r_b(t)$, according to eq 2:

$$r(t) = f_e(t)r_e(t) + f_b(t)r_b(t) \tag{2}$$

where the fractional contribution of exposed probes to the fluorescence anisotropy at time t, $f_e(t)$, is given by

$$f_e(t) = \frac{x_e\sum_{i=1}^{N_e}\alpha_{ie}\exp(-t/\tau_{ie})}{x_e\sum_{i=1}^{N_e}\alpha_{ie}\exp(-t/\tau_{ie}) + x_b\sum_{i=1}^{N_b}\alpha_{ib}\exp(-t/\tau_{ib})} \tag{3}$$

where τ_{ie}, α_{ie}, N_e, and x_e are the fluorescence lifetimes, decay amplitudes, number of decay components, and ground-state mole fraction of the exposed dansyl probes, respectively. The corresponding parameters for the buried probes are denoted by a b subscript. An analogous expression was used to represent the fractional contribution of the buried probes, $f_b(t)$.

The anisotropy decay for the exposed dansyl probes is the sum of contributions due to local rotation and overall tumbling:

$$r_e(t) = \beta_{1e}\exp(-t/\phi_{1e}) + \beta_{2e}\exp(-t/\phi_{2e}) \tag{4}$$

where β_{1e} and ϕ_{1e} are the anisotropy amplitude and decay time for local rotation ($\phi_{1e} \approx 1$ ns), respectively, and β_{2e} and ϕ_{2e} are the corresponding quantities for overall tumbling ($\phi_{2e} \approx 57$ ns), respectively. A similar expression was used to represent the time-dependent anisotropy of the buried dansyl probes.

The formalism outlined above does not allow for convolution of the instrument response function. However, in this work, convolution effects are considered to be negligible, given the extremely narrow width of the instrument response function (45 ps fwhm) and the time scale of the motions involved (≥1 ns). The fractions of buried and exposed dansyl probes were obtained by globally fitting 36 time-

Chart 1: Duplex DNA Sequences[a]

17*/27-mer	5′-TCGCAGCCGXCAAAATG AGCGTCGGCAGTTTTACATATAGCCGA-5′
17*/27G-mer	5′-TCGCAGCCGXCAAAATG AGCGTCGGCAGTTTTA$_{G}$ATATAGCCGA-5′
17*/27GG-mer	5′-TCGCAGCCGXCAAAATG AGCGTCGGCAGTTTT$_{GG}$ATATAGCCGA-5′
17*/27ATG-mer	5′-TCGCAGCCGXCAAAATG AGCGTCGGCAGTTT$_{ATG}$ATATAGCCGA-5′

[a] X denotes a deoxyuridine residue labeled at the 5 position with a dansyl probe.

resolved anisotropy decays, with the τ, α, and ϕ parameters for each probe population fixed at the values determined previously (*12*), and the β parameters linked across all data sets. The entire set of anisotropy decays was fitted simultaneously by optimizing the linked anisotropy amplitudes (β_{1e}, β_{2e}, β_{1b}, and β_{2b}) across all data sets, while at the same time, the fraction of buried probes (x_b) was optimized for each data set. The anisotropy decay data obtained for the D501A mutant protein were also analyzed separately. In all cases, the anisotropy data were assigned appropriate weighting factors according to the values of $I_{||}(t)$ and $I_{\perp}(t)$ at each time point (*19*). The quality of the fits was judged by the global reduced χ^2 value and the local reduced χ^2 values for each data set.

In eq 3, the fraction x_b corresponds to the fraction of DNA substrates bound to the 3′−5′ exonuclease site of the enzyme at equilibrium, and x_e ($x_e = 1 - x_b$) corresponds to the fraction of DNA bound to the polymerase site. Therefore, the equilibrium constant for partitioning of DNA from the polymerase site to the 3′−5′ exonuclease site, K_{pe}, was computed as

$$K_{pe} = \frac{x_b}{x_e} \tag{5}$$

As x_b becomes large, the value of K_{pe} becomes poorly defined, and any measured fraction of >0.95 was reported as a K_{pe} of ≥19. It should be noted that K_{pe} describes the equilibrium distribution of DNA substrates in the polymerase and 3′−5′ exonuclease sites and does not distinguish between intra- and intermolecular mechanisms of forming the corresponding DNA−protein complexes.

RESULTS

Fluorescence Anisotropy Decays of Dansyl-Labeled DNA Bound to Mutant Derivatives of Klenow Fragment. Time-resolved fluorescence anisotropy decays were recorded for dansyl-labeled primer−template oligonucleotides bound to various mutant derivatives of Klenow fragment. Nine mutant enzymes were examined, and four different primer−templates were used as substrates in each case. Details of the specific mutations are given later. The DNA substrates (Chart 1) were either perfectly base-paired (17*/27-mer), contained a single preformed G·G mismatch at the primer 3′ terminus (17*/27G-mer), or contained two or three consecutive 3′ terminal mismatches (17*/27GG-mer and 17*/27ATG-mer, respectively). The presence of mismatches is expected to favor binding of the DNA substrates at the 3′−5′ exonuclease site (*12*). In each case, the dansyl probe was attached to a deoxyuridine residue located seven bases upstream from the primer 3′ terminus, a position that previously was shown to experience different local environments according to whether the primer terminus was bound at the polymerase site or the 3′−5′ exonuclease site of Klenow fragment (*12*, *13*). Typical fluorescence anisotropy decay profiles for the four dansyl-labeled substrates bound to one of the mutant enzymes, the D424A mutant (Asp to Ala at position 424), are shown in Figure 2A. The corresponding decays for the F473A/D424A double mutant enzyme are shown in Figure 2B. It is evident that the

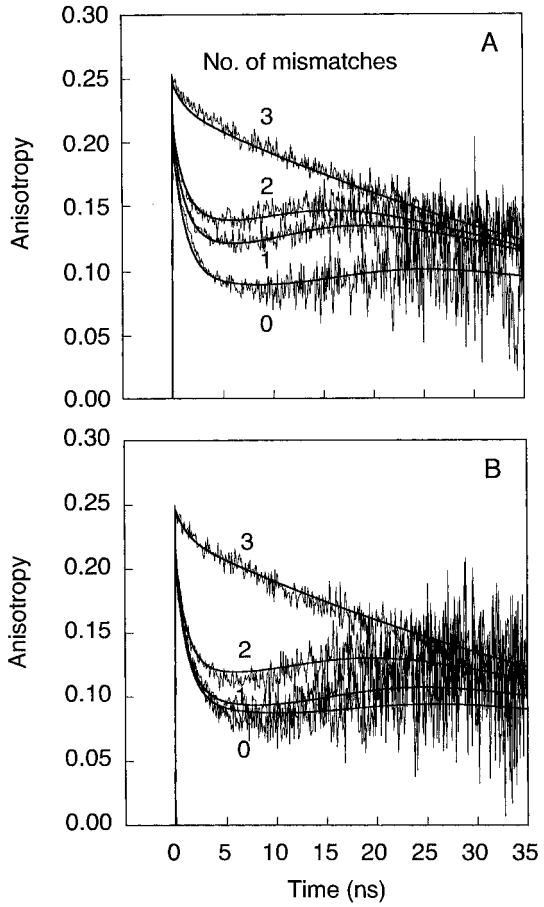

FIGURE 2: Fluorescence anisotropy decay profiles of dansyl-labeled DNA substrates bound to Klenow fragment. (A) Complexes of D424A Klenow fragment with, from top to bottom, 17*/27ATG-mer (three consecutive mismatches at the 3′ terminus), 17*/27GG-mer (two consecutive terminal mismatches), 17*/27G-mer (single G·G mismatch at the 3′ terminus), and 17*/27-mer (fully base-paired duplex). The fitted curves (solid lines) were obtained from a global fit of 36 data sets to a two-state model (eq 2), as described in the text. The fitted fractions of buried dansyl probes, equivalent to the fractions of exonuclease-bound DNA, and the reduced χ^2 values recovered for each data set are as follows: 17*/27ATG-mer, $x_b = 0.996$, $\chi_r^2 = 1.31$; 17*/27GG-mer, $x_b = 0.301$, $\chi_r^2 = 1.46$; 17*/27G-mer, $x_b = 0.221$, $\chi_r^2 = 1.05$; and 17*/27-mer, $x_b = 0.059$, $\chi_r^2 = 1.15$. (B) Complexes of the F473A/D424A double mutant Klenow fragment with the same set of duplex DNA substrates. Anisotropy decay profiles are labeled as in panel A, and the fitted curves (solid lines) were obtained from the same global analysis. The fitted fractions of buried dansyl probes and reduced χ^2 values recovered for each data set are as follows: 17*/27ATG-mer, $x_b = 0.970$, $\chi_r^2 = 1.24$; 17*/27GG-mer, $x_b = 0.179$, $\chi_r^2 = 1.17$; 17*/27G-mer, $x_b = 0.074$, $\chi_r^2 = 1.16$; and 17*/27-mer $x_b = 0.042$, $\chi_r^2 = 1.39$.

anisotropy decay of the dansyl probe is sensitive to both mismatches in the DNA substrates and mutations within the enzyme. In general, each DNA−protein complex exhibits a distinct anisotropy decay profile, indicating that the dansyl probe experiences a different environment, or distribution of environments, in each case.

To test whether the heterogeneous probe populations could be represented by two states of the dansyl probe, fluorescence anisotropy decay profiles for the entire set of 36 DNA−protein complexes were globally fitted to a two-state model of exposed and buried dansyl probes, as described in Materials and Methods. The fluorescence lifetimes of the exposed and buried dansyl probe were assigned different values, reflecting differences in the polarity of the surrounding environment. The values used are as follows: $\tau_{1e} = 1.01$ ns, $\tau_{2e} = 4.13$ ns, $\tau_{3e} = 11.9$ ns, $\tau_{1b} = 3.06$ ns, and $\tau_{2b} = 18.4$ ns (the corresponding amplitudes are $\alpha_{1e} = 0.30$, $\alpha_{2e} = 0.67$, $\alpha_{3e} = 0.03$, $\alpha_{1b} = 0.70$, and $\alpha_{2b} = 0.30$). The multiple lifetimes for each population reflect the nonexponential decay of the dansyl emission. These fluorescence decay parameters were determined in a previous work (*12*). The rotational correlation times for the two probe populations also were fixed at the values determined previously ($\phi_{1e} = \phi_{1b} = 1.2$ ns and $\phi_{2e} = \phi_{2b} = 57$ ns). The set of 36 anisotropy decays was fitted by optimizing the values of the linked anisotropy amplitudes across all data sets, while simultaneously adjusting the fraction of buried probes for each data set. In the case of the D501A mutant protein, the anisotropy decay data were also analyzed separately. An excellent global fit was obtained (global reduced $\chi^2 = 1.25$), and the reduced χ^2 values for the individual data sets were between 1.0 and 1.5. Furthermore, the fitted values for the anisotropy amplitudes of each probe population ($\beta_{1e} = 0.124$, $\beta_{2e} = 0.086$, $\beta_{1b} = 0.022$, and $\beta_{2b} = 0.228$) are in close agreement with the values determined in a previous study (*12*). These results confirm that the heterogeneous probe populations can be adequately modeled by two states, one state permitting extensive local motion of the probe and a second state with restricted motion of the dansyl probe. These two states of the dansyl probe correspond to DNA substrates bound at the polymerase and 3′−5′ exonuclease sites, respectively (*12*).

Mutations in the Carboxylate Ligands to the Metal Ions. We examined previously characterized derivatives of Klenow fragment having alanine substitutions at each of the carboxylate side chains that are seen crystallographically to coordinate two divalent metal ions at the 3′−5′ exonuclease site (*4*, *11*) (Figure 1). One metal ion (designated A) is bound to the protein by the side chains of Asp355, Glu357, and Asp501, while the other metal ion (designated B) shares the Asp355 side chain with the A site and is also coordinated by the side chain of Asp424 (*3*, *9*). The alanine substitutions cause a substantial decrease in 3′−5′ exonuclease activity (10^4−10^5-fold for the D355A, D424A, and D501A mutations and almost 10^3-fold for E357A), ensuring that the DNA substrates were not degraded during the course of the fluorescence measurements. A double mutant derivative containing both the E357A and D424A mutations was also examined.

The partitioning constant, K_{pe}, describing the distribution of DNA between the polymerase and 3′−5′ exonuclease sites was determined for each mutant enzyme bound to each of the four dansyl-labeled substrates, on the basis of the fitted fractions of exposed and buried probes recovered from the global analysis of the fluorescence anisotropy decay data (eq 5). For the fully base-paired substrate (17*/27-mer), the K_{pe} values are small for each mutant protein, indicating that the DNA strongly prefers to bind at the polymerase site in each case (Table 1). Accordingly, it is not possible to discern differences in partitioning due to mutations at the 3′−5′ exonuclease site. The presence of one or two mismatches within the DNA substrates results in greater occupancy of the 3′−5′ exonuclease site, such that the partitioning constants are different for each mutant enzyme (Table 1). For the single-mismatch substrate (17*/27G-mer), the K_{pe} value is largest for the D424A protein, is somewhat smaller

Table 1: Partitioning of DNA between Polymerase and 3′−5′ Exonuclease Sites

DNA name[a]	mutations[b]	K_{pe}[c]
17*/27-mer	D355A	0.045
-AATG	D501A	0.063 (0.046)[d]
-TTACA-	E357A	0.054
	D424A	0.063
	E357A/D424A	0.044
	L361A/D424A	0.058
	F473A/D424A	0.043
	Y497A/D424A	0.044
	H660A/D424A	0.057
17*/27G-mer	D355A	0.204
-AATG	D501A	0.172 (0.190)[d]
-TTA$_G$A-	E357A	0.114
	D424A	0.283
	E357A/D424A	0.097
	L361A/D424A	0.057
	F473A/D424A	0.075
	Y497A/D424A	0.400
	H660A/D424A	0.137
17*/27GG-mer	D355A	0.475
-AATG	D501A	0.412 (0.594)[d]
-TT$_{GG}$A-	E357A	0.301
	D424A	0.431
	E357A/D424A	0.290
	L361A/D424A	0.211
	F473A/D424A	0.257
	Y497A/D424A	0.511
	H660A/D424A	0.266
17*/27ATG-mer	D355A	≥19
-AATG	D501A	2.2 (≥19)[d]
-T$_{ATG}$A-	E357A	≥19
	D424A	≥19
	E357A/D424A	≥19
	L361A/D424A	≥19
	F473A/D424A	≥19
	Y497A/D424A	≥19
	H660A/D424A	≥19

[a] The bases near the 3′ terminus of each primer−template are included below the DNA name. See Chart 1 for complete DNA sequences. [b] Mutations are abbreviated using the following convention: The residue number is preceded by the one-letter code for the wild-type amino acid and followed by the code for the mutant amino acid. [c] Equilibrium constant for partitioning of DNA between polymerase and 3′−5′ exonuclease sites, determined from a global fit of fluorescence anisotropy decays using a common set of probe parameters for each DNA−protein complex, unless otherwise indicated. See the text for details. K_{pe} values are the average of at least two determinations. Errors are ±10% of the value obtained. [d] Values in parentheses were determined from a global fit of anisotropy decays obtained for the D501A mutant protein only. The anisotropy amplitudes and fractions of buried probes were optimized separately from other data sets. See the text for details.

for the D355A and D501A proteins, and is significantly smaller for the E357A protein. These results indicate that the E357A mutation reduces the partitioning of the mismatched DNA into the 3′−5′ exonuclease site relative to mutations of the other carboxylate side chains. In the case of the double-mismatch DNA substrate (17*/27GG-mer), the K_{pe} values are larger for each of the mutant enzymes, reflecting the greater tendency of the DNA to bind at the 3′−5′ exonuclease site, but the smallest value is again seen for the E357A mutant protein (Table 1). Taken together, these results suggest that the Glu357 side chain is important for binding DNA substrates at the 3′−5′ exonuclease site.

To assess further the contribution of Glu357, K_{pe} values were also determined for the E357A/D424A double mutant enzyme (Table 1). Assuming that the effects of mutations are additive, these values can be directly compared with the corresponding data for the D424A mutant, thereby isolating the effect of the E357A mutation on the partitioning of the DNA substrates between the polymerase and 3′−5′ exonuclease sites. Thus, in the case of the single-mismatch DNA substrate, comparison of the relevant K_{pe} values in Table 1 indicates that the removal of the Glu357 side chain reduces the partitioning of DNA into the 3′−5′ exonuclease center by a factor of 2.9.

The partitioning data for the E357A/D424A mutant enzyme can also be compared with corresponding data for the E357A mutant. In this case, differences in the K_{pe} values for the two proteins can be attributed to the D424A mutation, again under the assumption that the effects of each mutation are additive. In fact, the results in Table 1 indicate that the partitioning constants for complexes of the 17*/27G-mer substrate with the E357A/D424A or E357A mutant enzyme are very similar, indicating that the D424A mutation has relatively little additional effect on the partitioning of this DNA. The same is true of the other DNA substrates (Table 1). It appears, therefore, that the D424A mutation has the least effect on partitioning of any of the carboxylate mutations. It should be noted that the K_{pe} values for the 17*/27-mer and 17*/27G-mer substrates bound to the D424A mutant protein are somewhat smaller than those reported for the same DNA sequences (referred to as 17*TG·27B-C and 17*TG·27B-G, respectively) in a previous study (*12*). It seems likely that the previous measurements overestimated the partitioning constants for these two primer−templates, possibly due to problems in the synthesis of the original 17*TG·27B-C and 17*TG·27B-G oligonucleotides. We note that the present results for the 17*/27-mer and 17*/27G-mer substrates are reproducible in two independent DNA preparations and for multiple preparations of the D424A protein.

The anisotropy decay profiles obtained for the triple-mismatch DNA substrate (17*/27ATG-mer) are similar for the D424A, D355A, and E357A mutant enzymes and indicate that the DNA is bound predominantly (>95%) at the 3′−5′ exonuclease site in each case. This is also true of the E357A/D424A mutant enzyme. The corresponding K_{pe} values are reported as lower limits (Table 1). These results are consistent with previous observations showing that DNA primer−templates containing multiple consecutive mismatches are bound predominantly at the 3′−5′ exonuclease site of Klenow fragment (*12*). For the D501A mutant, however, the anisotropy decay profile for the triple-mismatch DNA substrate exhibits a more rapid initial decay (not shown) and the recovered fraction of buried probes is significantly smaller ($x_b = 0.68$) than those for the other mutant enzymes, implying that the DNA is still partly bound at the polymerase site or that some of the DNA is free in solution. To eliminate this latter possibility, the 17*/27ATG-mer substrate was titrated with increasing amounts of the D501A mutant protein and it was observed that the anisotropy decay profile remained constant. Moreover, the results obtained for the D501A mutant are reproducible in two independent protein preparations. Alternatively, the triple-mismatch substrate may in fact be bound mostly at the 3′−5′ exonuclease site, but the structure of that site may have changed in such a way that the local environment of the buried dansyl probes is altered, resulting in the different anisotropy decay profile. To test this possibility, a separate global analysis was performed using only the data sets obtained for the D501A protein (with all four DNA substrates). The resulting values for the anisotropy amplitudes of the buried probes ($\beta_{1b} = 0.034$ and $\beta_{2b} = 0.195$) are different from the values obtained from the original global analysis ($\beta_{1b} = 0.022$ and $\beta_{2b} = 0.228$), whereas the remaining spectroscopic parameters are essentially the same in both analyses. Moreover, the recovered fraction of buried probes for the triple-mismatch substrate in this analysis ($x_b > 0.95$) indicates that the DNA is indeed bound mostly at the 3′−5′ exonuclease site, as observed for the binding of this DNA substrate to each of the other mutant enzymes. Thus, it appears that the D501A mutant does have a different structure than the other mutant enzymes, resulting in a different environment for the buried dansyl probes. On the basis of the anisotropy amplitudes, it appears that the buried dansyl probes observed for DNA substrates bound to the D501A mutant are somewhat less restricted in their local motion than those for any of the other DNA−protein complexes. Nonetheless, this change in the buried probe environment is accounted for in the refined K_{pe} values shown in parentheses in Table 1.

Mutations in Residues That Contact the DNA Substrate. We examined a group of residues (Leu361, Phe473, Tyr497, and His660) that have been shown crystallographically to be in close proximity to a DNA 3′ terminus bound at the 3′−5′ exonuclease site of Klenow fragment (*3*, *9*) (Figure 1). Alanine substitutions of Leu361, Phe473, and Tyr497 have been described previously (*11*, *14*); the alanine replacement of His660, a residue within the polymerase domain, was constructed following procedures established in earlier studies of polymerase domain mutants (*15*). Aside from F473A, which caused a (3×10^4)-fold decrease in 3′−5′ exonuclease activity, the other mutant proteins had substantial levels of 3′−5′ exonuclease activity [L361A and Y497A reduced the activity by about 20-fold; H660A was similar to wild type (C. M. Joyce, unpublished observations)]. All four mutations were combined with the D424A mutation, which essentially abolishes 3′−5′ exonuclease activity (*4*), to prevent exonuclease degradation of the dansyl-labeled DNA substrates during the fluorescence measurements and to allow a comparison of the binding properties of the double mutant enzymes with the single D424A mutant as a control.

Typical fluorescence anisotropy decay profiles for the four dansyl-labeled DNA substrates bound to one of the mutant enzymes (F473A/D424A) are presented in Figure 2B.

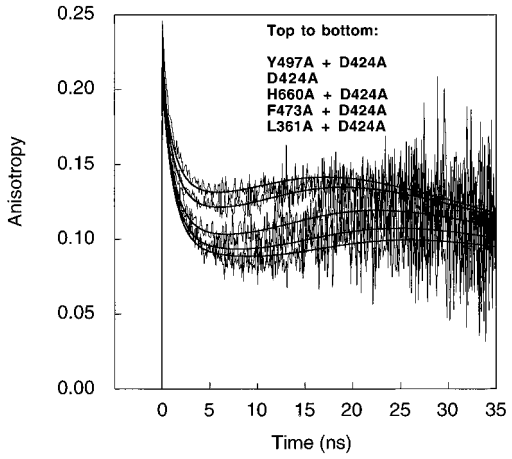

FIGURE 3: Fluorescence anisotropy decay profiles of the single-mismatch DNA duplex (17*/27G-mer) bound to various mutant derivatives of Klenow fragment. The mutant enzymes used are (from top to bottom) Y497A/D424A (x_b = 0.284, χ_r^2 = 1.19), D424A (x_b = 0.221, χ_r^2 = 1.05), H660A/D424A (x_b = 0.120, χ_r^2 = 1.17), F473A/D424A (x_b = 0.074, χ_r^2 = 1.16), and L361A/D424A (x_b = 0.054, χ_r^2 = 1.15). The values indicated in parentheses are the fractions of buried dansyl probes, equivalent to the fraction of DNA bound at the 3′−5′ exonuclease site, and the reduced χ^2 values for each data set, obtained from a global fit (solid lines) to 36 data sets, as described in the text.

Comparison of these data with the corresponding anisotropy profiles for the D424A mutant (Figure 2A) reveals that the additional F473A mutation in the double mutant enzyme has a significant effect upon the anisotropy decay profiles for the DNA substrates containing one or two mismatches (17*/27G-mer and 17*/27GG-mer, respectively). Figure 3 presents a direct comparison of the anisotropy decay profiles for complexes of the 17*/27G-mer substrate with each of the mutant enzymes and with the D424A mutant. It is obvious that the anisotropy decay for each double mutant enzyme is different from that obtained for the "reference" derivative containing only the D424A mutation. This observation indicates that mutation of Leu361, Phe473, Tyr497, or His660 alters the partitioning of DNA between the polymerase and 3′−5′ exonuclease sites of Klenow fragment.

To quantify the contribution of each side chain to the partitioning of the DNA substrates between the polymerase and 3′−5′ exonuclease sites, equilibrium partitioning constants were evaluated for each mutant enzyme from the global analysis of the fluorescence anisotropy decay data. As in the case of the carboxylate mutants, the DNA substrates containing one or two terminal mismatches are the most sensitive to mutations within the enzyme (Table 1). For the DNA substrate containing a single mismatch (17*/27G-mer), the K_{pe} value for the L361A/D424A mutant enzyme is significantly smaller (0.057) than the corresponding value for the D424A mutant (0.283). Assuming that the effects of the mutations are additive, these results indicate that the removal of the Leu361 side chain in the double mutant enzyme reduces the partitioning of DNA into the 3′−5′ exonuclease site by a factor of 5.0. A similar analysis of the F473A/D424A and H660A/D424A mutant enzymes indicates that the removal of the Phe473 or His660 side chains reduces the K_{pe} values for the 17*/27G-mer DNA substrate by factors of 3.8 and 2.1, respectively. Similar trends are observed for the double-mismatch substrate (17*/27GG-mer) bound to each of the mutant enzymes, although the overall K_{pe} values are larger (Table 1). It is important to note that the DNA duplexes are fully bound to the mutant enzymes in all the measurements reported here, as detailed in Materials and Methods. Thus, the smaller K_{pe} values measured for the mutant enzymes relative to the D424A derivative reflect a change in the partitioning of DNA between the polymerase and 3′−5′ exonuclease sites, as assumed here, rather than a partial dissociation of DNA from the enzyme.

Interestingly, the K_{pe} value for binding of the single-mismatch DNA substrate to the Y497A/D424A mutant enzyme is *larger* than the corresponding value for the D424A mutant (Table 1). A similar effect is observed for the double-mismatch DNA substrate. These results suggest that the removal of the side chain of Tyr497 actually favors the binding of these DNAs to the 3′−5′ exonuclease site over binding to the polymerase site.

DISCUSSION

We have quantified the contribution of individual amino acid residues to the partitioning of DNA substrates between the polymerase and 3′−5′ exonuclease active sites of Klenow fragment. The experimental approach employed here to probe the DNA partitioning equilibrium is based on measurements of the time-resolved fluorescence anisotropy decay of dansyl-labeled DNA substrates bound to the enzyme. In a previous study, it was demonstrated that the anisotropy decay of the dansyl probe could be represented in terms of two distinct populations, a protein-bound state in which the probe was relatively solvent-exposed and a buried state in which the probe was in more intimate contact with the protein (*12*). The buried probes were characterized by long emission lifetimes and restricted local motion. The buried population was observed to increase as mismatches were introduced into the DNA substrates, with a corresponding decrease in the exposed dansyl probes, suggesting that the buried probes correspond to DNA primer−templates bound at the 3′−5′ exonuclease site of the enzyme while the exposed dansyl probes represent DNA at the polymerase site. This assignment is confirmed by the results of this study, which show that the population of buried dansyl probes is also sensitive to mutations within the 3′−5′ exonuclease site. In addition, the assignment of the two probe populations is consistent with previous studies in which an epoxy-AMP residue at the primer terminus was used to anchor the DNA substrate at the polymerase site, resulting in a homogeneous population of exposed dansyl probes (*13*). The fractions of dansyl probes in the two environments are reflected in the shape of the anisotropy decay profile, allowing for the direct quantitation of the partitioning of DNA substrates between the polymerase and 3′−5′ exonuclease sites. This partitioning is described by the internal equilibrium constant, K_{pe}.

In this study, we have extended this approach to investigate the effect of protein mutations on the DNA partitioning equilibrium. We studied mutations in amino acid residues that are seen by X-ray crystallography to be close to the 3′ terminus of a DNA substrate bound to the 3′−5′ exonuclease site (Figure 1). For each mutant derivative of Klenow fragment, a series of DNA substrates containing various numbers of preformed mismatches (zero to three) were

examined, since these were expected to partition differently between the polymerase and 3′−5′ exonuclease sites. Thus, the effects of mutations on the partitioning were examined under a variety of conditions. The use of the different mismatched DNA substrates also facilitated the global analysis procedure used to treat the fluorescence anisotropy decays. In the case of the fully base-paired substrate (17*/27-mer), the fluorescence anisotropy decay was similar for each mutant protein, reflecting a predominant population of exposed dansyl probes. This observation is in agreement with previous studies showing that a fully base-paired primer−template prefers to bind at the polymerase site, reflecting the intrinsic affinity of that site for double-stranded DNA (*12*). Accordingly, the matched substrate is not sensitive to mutations at the 3′−5′ exonuclease site. In addition, the triple-mismatch DNA substrate (17*/ATG-mer) exhibited a similar anisotropy decay pattern, indicative of a homogeneous population of buried dansyl probes, when bound to any of the mutant proteins (except the D501A protein, discussed later), showing that this DNA was bound predominantly at the 3′−5′ exonuclease site in all cases. The strong preference of multiple mismatched DNA for the 3′−5′ exonuclease site arises from weaker binding at the polymerase site combined with an increased melting capacity of the duplex terminus (*12*). Accordingly, it was only possible to determine a lower limit for the equilibrium partitioning constants under these conditions, and any variations among the mutant proteins were outside the range of the assay.

In the case of the single-mismatch and double-mismatch DNA substrates (17*/27G-mer and 17*/27GG-mer, respectively), however, the fraction of buried dansyl probes was found to be different for each mutant enzyme. For these substrates, the partitioning equilibrium is poised between binding of the primer terminus at the polymerase site and at the 3′−5′ exonuclease site. Accordingly, changes in the partitioning of these substrates fall within the most sensitive range of the time-resolved fluorescence assay, allowing for the quantitation of subtle changes in the energetics of DNA−protein interactions at the 3′−5′ exonuclease site due to the various mutations under study. Interestingly, the K_{pe} values for the single- and double-mismatch substrates differ by only a factor of 2−3, whereas a previous study found a much larger difference in the partitioning of primer−templates containing a single G·G mismatch or two consecutive G·G mismatches (*12*). The double-mismatch substrate used in this study has a T(primer)·G(template) mismatch at the penultimate position, which may be less destabilizing than a G·G mismatch. In fact, T·G mismatches are among the most commonly formed mispairs in vivo (*20*), suggesting that they are better tolerated in DNA than other mismatches.

To quantify the effect of a specific mutation, it is necessary to compare the partitioning of a DNA substrate bound to wild-type Klenow fragment and to the mutant enzyme of interest. Unfortunately, the wild-type Klenow fragment could not be examined in our studies since this enzyme would degrade the DNA substrates, and thus, we cannot compare the mutant enzymes to the wild-type enzyme directly. Instead, we have compared the mutant enzymes to the exonuclease-deficient D424A mutant which shows the smallest defects in partitioning DNA from polymerase to 3′−5′ exonuclease sites. This choice is based on the observation that the E357A single mutant and E357A/D424A double mutant enzymes exhibit very similar K_{pe} values for a variety of DNA substrates (Table 1). Since these two mutant enzymes only differ at a single position, namely at residue 424, it appears that the alanine replacement of Asp424 has very little additional effect on the partitioning of DNA substrates between the polymerase and 3′−5′ exonuclease sites.

The absence of any significant changes in the partitioning of DNA substrates due to the D424A mutation also provides information on the role of the divalent metal ions at the 3′−5′ exonuclease site. Previous studies have shown that the D424A mutation results in the loss of one of the two metal ions (metal B) at the 3′−5′ exonuclease site (*4*). Since the D424A mutation has little effect on the partitioning of DNA substrates, it appears that metal B does not contribute significantly to the binding of DNA at the 3′−5′ exonuclease site. Metal B, however, does play an important role in the catalysis of the 3′−5′ exonuclease reaction (*4*, *11*), implying that the interaction between metal B and the DNA substrate occurs in the transition state rather than in the ground state.

Our results indicate that the other metal ion at the 3′−5′ exonuclease site (metal A) does play a role in binding the DNA substrate. Metal A is bound to the protein by the side chains of Asp355, Asp501, and Glu357 (*3*, *9*). Mutation of the Asp355 side chain results in the loss of metal A but has no effect on the binding of metal B (*6*). The K_{pe} value for binding the single-mismatch DNA substrate is smaller for the D355A mutant enzyme than for the D424A mutant (Table 1), indicating that the D355A mutant is less proficient in binding DNA at the 3′−5′ exonuclease site. This difference can be attributed to the loss of metal A in the D355A mutant enzyme, rather than to the absence of a DNA−protein contact, because the Asp355 side chain does not appear to interact directly with the DNA substrate (*9*). Our data indicate, therefore, that metal A makes a small contribution to binding the DNA substrate at the 3′−5′ exonuclease site. The involvement of metal A in substrate binding is also consistent with crystallographic data indicating that the oxygen atoms of the 3′ terminal phosphate group interact with metal A (*9*), and is consistent with the results of an earlier mutagenesis study (*4*). In addition, our data indicate that the removal of the Asp501 side chain also reduces the partitioning of the single-mismatch DNA into the 3′−5′ exonuclease site, to the same extent as observed for the D355A mutant protein (Table 1). This effect probably also reflects the loss of metal A from the 3′−5′ exonuclease site. In the case of the double-mismatch DNA substrate, however, the K_{pe} values for the D355A and D501A mutant enzyme are similar to that observed for the D424A mutant (Table 1), indicating that the absence of metal A has little effect on partitioning of this DNA from the polymerase site to the 3′−5′ exonuclease site. These results suggest that the small defect caused by the loss of metal A in the D355A and D501A mutant enzymes is masked by the stronger preference of a doubly mismatched substrate to bind at the 3′−5′ exonuclease site.

Our results suggest that Glu357 also is involved in binding DNA to the 3′−5′ exonuclease site. The K_{pe} value obtained for the single-mismatch DNA substrate bound to the E357A/D424A mutant enzyme is smaller than the corresponding value for the D424A mutant, indicating that removal of the

Glu357 side chain reduces binding of DNA to the 3′−5′ exonuclease site by a factor of 2.9 (Table 1). Crystallographic studies of Klenow fragment−DNA complexes indicate that the side chain of Glu357 serves as one of the ligands to metal A and is also hydrogen-bonded to the 3′-hydroxyl of the DNA substrate (*4*, *9*). Therefore, removal of the side chain eliminates a direct DNA−protein contact and could also disrupt binding of metal A. Both effects could potentially weaken DNA binding at the 3′−5′ exonuclease site. Our results (Table 1) show, however, that the E357A mutation has a greater effect on the partitioning equilibrium than expected simply on the basis of removing metal A (exemplified by the D355A and D501A proteins). In fact, biochemical studies indicate that metal A is actually retained in the E357A mutant protein (*11*). Therefore, the shift in the DNA partitioning equilibrium resulting from the E357A mutation presumably reflects the loss of a direct DNA−protein contact. Our results lend support to the proposal that the side chain of Glu357 is involved primarily in binding the DNA substrate at the 3′−5′ exonuclease site.

Mutations of the Leu361 and Phe473 side chains produced the largest effects of any of the mutations examined in this study. The L361A mutation reduces the partitioning of the single-mismatch DNA into the 3′−5′ exonuclease site by a factor of 5.0, as can be seen by comparing the K_{pe} values obtained for the L361A/D424A and D424A proteins (Table 1). Similarly, the F473A mutation reduces this partitioning by a factor of 3.8. Thus, the side chains of Leu361 and Phe473 are important for binding the DNA substrate to the 3′−5′ exonuclease site, consistent with structural data showing that the side chain of Phe473 is stacked on the 3′ terminal base of the primer strand and the side chain of Leu361 is wedged between the terminal and penultimate bases (*6*, *9*) (Figure 1). To gain an appreciation of the energies associated with these interactions, the change in free energy of the exonuclease-bound DNA complex relative to the polymerase-bound complex was calculated from the partitioning constants, using the relationship

$$\Delta\Delta G = -RT \ln[K_{pe}(\text{mut})/K_{pe}(\text{D424A})]$$

where K_{pe}(mut) is the partitioning constant for the relevant mutant enzyme (L361A/D424A or F473A/D424A) and K_{pe}(D424A) is the corresponding value for the D424A mutant used as a reference, each bound to a common DNA substrate (17*/27G-mer). The ΔΔG values for removal of the Leu361 and Phe473 side chains are 3.9 and 3.2 kJ mol^{-1}, respectively. These values are in an appropriate range for hydrophobic contributions to DNA−protein binding. For example, the energy contributed to DNA−protein binding by a single methyl group has been determined to be in the range of 4.6−5.9 kJ mol^{-1} for the endonucleases *Eco*RV (*21*) and *Rsr*I (*22*). The somewhat smaller energies found for the side chains of Leu361 and Phe473 may reflect the requirement of the 3′−5′ exonuclease site to bind an arbitrary sequence of nucleotides, such that the complementarity between molecular surfaces is less optimal than in the highly sequence-specific interaction of a restriction endonuclease with its target DNA sequence.

A similar free energy analysis shows that the removal of the side chain of Glu357 destabilizes binding of DNA at the 3′−5′ exonuclease site by 2.6 kJ mol^{-1}. As noted earlier, crystallographic data indicate that Glu357 is hydrogen-bonded to the 3′-hydroxyl group of the DNA substrate at the exonuclease site (*4*). Interestingly, the energetic contribution of the Glu357 side chain is less than expected for a single DNA−protein hydrogen bond, which ranges between 3.8 and 7.1 kJ mol^{-1} for a variety of restriction endonucleases (*21*−*23*). This may reflect the fact that one of the oxygens of Glu357 is also used to ligate metal A, which could weaken the hydrogen bond with the DNA hydroxyl group by reducing the electron density on the remaining oxygen of Glu357.

In addition to the residues that interact with the primer 3′ terminus at the 3′−5′ exonuclease site, we have also examined His660, a side chain from the polymerase domain that interacts with the third base from the 3′ end (*9*) (Figure 1). The H660A mutation also reduces the partitioning of DNA into the 3′−5′ exonuclease site, as reflected in the smaller K_{pe} value for the H660A/D424A mutant enzyme relative to the D424A mutant, each complexed with the single-mismatch DNA substrate (Table 1). The corresponding $\Delta\Delta G$ value for removal of the side chain of His660 is 1.8 kJ mol^{-1}, significantly less than the energies associated with the Leu361 and Phe473 side chains. On the basis of these results, it is evident that His660 helps to stabilize the DNA substrate at the 3′−5′ exonuclease site, consistent with structural data showing that this residue interacts with the primer strand upstream from the point of hydrolysis (*9*). However, the contacts made by His660 appear to be less important in energetic terms than the interactions involving the 3′ terminal base.

The conclusions presented above rest upon the comparison of the equilibrium partitioning constants determined for different mutant enzymes bound to a common DNA substrate. Inherent in such comparisons is the assumption that the mutant enzymes have the same overall structure, except at the positions of the altered amino acids. Crystallographic studies have shown this to be true for the D424A protein and a D355A/E357A double mutant derivative of Klenow fragment (*4*). In addition, Derbyshire et al. (*11*) have presented circumstantial evidence that other mutations within the exonuclease domain do not perturb the overall structure of the enzyme. Therefore, in assessing the results for the various mutant enzymes examined here, it is reasonable to ascribe differences in the partitioning of DNA between polymerase and 3′−5′ exonuclease sites to the absence of specific amino acid side chains. This is supported by the fact that the majority of the anisotropy decay data can be readily fitted in terms of a single two-state model using a common set of spectroscopic parameters to describe the two environments of the dansyl probe. In view of the strong environmental dependence of the dansyl emission (*18*), this implies that the two binding modes (the polymerase mode and the exonuclease mode) are similar for each DNA−protein complex. The only exception is the D501A mutant protein which appears to bind DNA substrates at the 3′−5′ exonuclease site in a somewhat different manner to all the other mutant enzymes, resulting in a different environment for the buried dansyl probes. It should be noted, however, that the resulting changes in the spectroscopic parameters of the buried probes are very small and the difference in the overall structure of the DNA−protein complex may be relatively minor. Nonetheless, it was still possible to estimate

the DNA partitioning constants for the D501A mutant protein by analyzing the anisotropy decays independently of the other proteins.

Our data for the Y497A/D424A mutant enzyme produced a surprising result. The partitioning constants for binding of this protein to single- and double-mismatch DNA substrates are significantly *larger* than the corresponding data for the D424A mutant, indicating that the DNA substrates bind more tightly to the 3′−5′ exonuclease site when the side chain of Tyr497 is removed. This result runs counter to the data for all the other mutant enzymes, which demonstrate that removal of a side chain from the 3′−5′ exonuclease site always causes less partitioning of DNA into that site. Structural data indicate that Tyr497 is hydrogen-bonded to the phosphate of the bond to be cleaved in the 3′−5′ exonuclease reaction (*3*) (Figure 1). Our results indicate that this interaction does not contribute to stabilizing the DNA bound at the 3′−5′ exonuclease site, showing that a crystallographically defined DNA−protein contact does not necessarily correspond to a favorable interaction energy. In fact, it appears that the interaction between the side chain of Tyr497 and DNA may actually be destabilizing for substrate binding, suggesting that this interaction plays a more subtle role in the 3′−5′ exonuclease reaction. For example, the Tyr497 side chain might orient the DNA substrate in a strained conformation that facilitates hydrolysis of the phosphodiester bond. This is consistent with the observation that replacement of the Tyr497 residue with alanine results in a significant loss of 3′−5′ exonuclease activity (*11*). Alternatively, the removal of the tyrosine side chain and the resulting stabilization of DNA binding may decrease the rate of dissociation of the primer 3′ terminus from the exonuclease site, which could also reduce the overall rate of hydrolysis.

The results presented in this paper on partitioning of DNA substrates between polymerase and 3′−5′ exonuclease active centers complement and extend the studies of other DNA polymerases. Previous studies of ϕ29 and T4 DNA polymerases have identified some amino acid residues that may affect the binding of DNA substrates to the polymerase or 3′−5′ exonuclease sites. For example, de Vega et al. (*24*) have characterized mutant derivatives of ϕ29 DNA polymerase that are defective in 3′−5′ exonucleolysis on double-stranded DNA substrates. The mutations affect two residues in the 3′−5′ exonuclease domain that appear to be involved in substrate binding, although the effects were not quantified in terms of changes in the partitioning of DNA between the polymerase and 3′−5′ exonuclease sites. Reha-Krantz and co-workers (*25*, *26*) have used genetic selection methods to identify mutations in T4 DNA polymerase that alter the balance between DNA polymerization and 3′−5′ exonucleolytic proofreading. Some of these mutations also affect residues within the 3′−5′ exonuclease domain, although it is not known whether the mutations directly affect the interaction of DNA with the exonuclease site. The spectroscopic technique described in this study provides a direct probe of DNA−protein interactions at the 3′−5′ exonuclease site and has been used to evaluate the energetic contributions of several amino acids that are in close proximity to the primer 3′ terminus. Moreover, the method could also be used to quantify interaction energies at the polymerase site of the enzyme, because the mutation of DNA contact residues within that site should also alter the partitioning of DNA within the enzyme and thereby change the fluorescence anisotropy decay profile of the dansyl probe. We anticipate that the time-resolved fluorescence anisotropy technique will provide a novel method for identifying important contact residues and dissecting the energetics of DNA−protein interactions associated with both binding modes of DNA polymerase.

ACKNOWLEDGMENT

C. M. Joyce thanks Xiaojun Chen Sun for help with plasmid constructs. We thank Chad Brautigam for help with the structure illustrations.

REFERENCES

1. Joyce, C. M., and Steitz, T. A. (1994) *Annu. Rev. Biochem. 63*, 777−822.
2. Ollis, D. L., Brick, P., Hamlin, R., Xuong, N. G., and Steitz, T. A. (1985) *Nature 313*, 762−766.
3. Freemont, P. S., Friedman, J. M., Beese, L. S., Sanderson, M. R. and Steitz, T. A. (1988) *Proc. Natl. Acad. Sci. U.S.A. 85*, 8924−8928.
4. Derbyshire, V., Freemont, P. S., Sanderson, M. R., Beese, L., Friedman, J. M., Joyce, C. M., and Steitz, T. A. (1988) *Science 240*, 199−201.
5. Brutlag, D., and Kornberg, A. (1972) *J. Biol. Chem. 247*, 241−248.
6. Beese, L., Derbyshire, V., and Steitz, T. A. (1993) *Science 260*, 352−355.
7. Cowart, M., Gibson, K. J., Allen, D. J., and Benkovic, S. J. (1989) *Biochemistry 28*, 1975−1983.
8. Hochstrasser, R. A., Carver, T. E., Sowers, L. C., and Millar, D. P. (1994) *Biochemistry 33*, 11971−11979.
9. Beese, L., and Steitz, T. A. (1991) *EMBO J. 10*, 25−33.
10. Eom, S. H., Wang, J., and Steitz, T. A. (1996) *Nature 382*, 278−281.
11. Derbyshire, V., Grindley, N. D. F., and Joyce, C. M. (1991) *EMBO J. 10*, 17−24.
12. Carver, T. E., Hochstrasser, R. A., and Millar, D. P. (1994) *Proc. Natl. Acad. Sci. U.S.A. 91*, 10670−10674.
13. Guest, C. R., Hochstrasser, R. A., Dupuy, C., Allen, D. J., Benkovic, S. J., and Millar, D. P. (1991) *Biochemistry 30*, 8759−8770.
14. Derbyshire, V., Pinsonneault, J. K., and Joyce, C. M. (1995) *Methods Enzymol. 262*, 363−385.
15. Polesky, A. H., Steitz, T. A., Grindley, N. D. F., and Joyce, C. M. (1990) *J. Biol. Chem. 265*, 14579−14591.
16. Sambrook, J., Fritsch, E. F., and Maniatis, T. (1989) *Molecular Cloning: A Labratory Manual*, Cold Spring Harbor Laboratory Press, Plainview, NY.
17. Joyce, C. M., and Derbyshire, V. (1995) *Methods Enzymol. 262*, 3−13.
18. Allen, D. J., Darke, P. L., and Benkovic, S. J. (1989) *Biochemistry 28*, 3612−3621.
19. O'Connor, D. V., and Phillips, D. (1984) *Time-Correlated Single Photon Counting*, p 271, Academic Press, London.
20. Echols, H., and Goodman, M. F. (1991) *Annu. Rev. Biochem. 60*, 477−511.
21. Newman, P. C., Williams, D. M., Cosstick, R., Seela, F., and Connolly, B. A. (1990) *Biochemistry 29*, 9902−9910.
22. Aiken, C. R., McLaughlin, L. W., and Gumport, R. I. (1991) *J. Biol. Chem. 266*, 19070−19078.
23. Lesser, D. R., Kurpiewski, M. R., and Jen-Jacobson, L. (1990) *Science 250*, 776−786.
24. de Vega, M., Lazaro, J. M., Salas, M., and Blanco, L. (1996) *EMBO J. 15*, 1182−1192.
25. Reha-Krantz, L. J., and Nonay, R. L. (1994) *J. Biol. Chem. 269*, 5635−5643.
26. Stocki, S. A., Nonay, R. L., and Reha-Krantz, L. J. (1995) *J. Mol. Biol. 254*, 15−28.
27. Humphrey, W., Dalke, A., and Schulten, K. (1996) *J. Mol. Graphics 14*, 33−38.

BI9720181